The Reduction Mechanism of a Natural Chromite at 1416 °C

O. SOYKAN, R.H. ERIC, and R.P. KING

The behavior of a natural chromite from the Bushveld Complex, Transvaal, South Africa, during reduction at 1416 °C by graphite was studied by means of thermogravimetric analysis, X-ray diffraction (XRD) analysis, energy-dispersive X-ray analysis (EDAX), and metallographic analysis. Experimental runs were allowed to proceed up to 120 minutes, resulting in 99 pct reduction. The specific objective of this study was to delineate the reduction mechanism of chromite by graphite. Zoning was observed in partially reduced chromites with degrees of reduction of up to about 70 pct. The inner cores were rich in iron, while the outer cores were depleted of iron. Energy-dispersive X-ray analysis revealed that Fe^{2+} and Cr^{3+} ions had diffused outward, whereas Cr^{2+}, Al^{3+}, and Mg^{2+} ions had diffused inward. The following mechanism of reduction, which is based on the assumption that the composition of the spinel phase remains stoichiometric with increasing degree of reduction, is proposed. (a) Initially, Fe^{3+} and Fe^{2+} ions at the surface of the chromite particle are reduced to the metallic state. This is followed immediately by the reduction of Cr^{3+} ions to the divalent state. (b) Cr^{2+} ions diffusing toward the center of the particle reduce the Fe^{3+} ions in the spinel under the surface of the particle to Fe^{2+} at the interface between the inner and outer cores. Fe^{2+} ions diffuse toward the surface, where they are reduced to metallic iron. (c) After the iron has been completely reduced, Cr^{3+} and any Cr^{2+} that is present are reduced to the metallic state, leaving an iron- and chromium-free spinel, $MgAl_2O_4$.

I. INTRODUCTION

CHROMITE ores comprise chromium spinels combined with physically separable gangue minerals. The chemical formula of chromium spinels can be represented as AB_2O_4, where A represents divalent cations (*i.e.*, Fe and Mg) in tetrahedral sites and B represents trivalent cations (*i.e.*, Cr, Al, and Fe) in octahedral sites. In some cases, tetravalent cations (*i.e.*, Ti) replace trivalent cations in octahedral sites, resulting in an ulvospinel. In the pure ulvospinel end member, Fe_2TiO_4, half the Fe^{2+} ions occupy tetrahedral sites, and the other half occupy octahedral sites. Each spinel unit cell comprises eight AB_2O_4 units, in which the cubic close packing of 32 oxygen atoms provides 64 tetrahedral cation sites, as well as 32 octahedral cation sites.[1] The distribution of the cations between the A and B sites gives rise to two structural types of spinel. Normal spinels have eight divalent cations in the tetrahedral sites and 16 trivalent cations in octahedral sites, *e.g.*, $Fe^{2+}(Cr^{3+})_2O_4$. Inverse spinels have eight of the 16 trivalent cations in tetrahedral sites, and the octahedral sites are occupied by eight trivalent and eight divalent cations. Magnetite, $Fe^{3+}(Fe^{2+}, Fe^{3+})O_4$, is an example of an inverse spinel. There are many spinels in which the distribution of cations lies between the two extremes of the normal and inverse structures.[2,3]

The reduction of any crystal requires the migration of atoms or ions, which is possible if imperfections are present in the lattice.[4] In chromite, the sublattice of the oxygen ion is almost perfect compared with that of the cation. This can be concluded from the almost complete dense packing and the relatively large radius of the oxygen ion, which is almost twice that of Fe^{2+} and Fe^{3+} ions. The known oxygen diffusion coefficients are several orders of magnitude smaller than the cation diffusion coefficients.[5,6] Due to the relatively large size of oxygen ions, the small diffusion coefficients, and the dense packing of the oxygen ion sublattice, during the initial stages of reduction, the oxygen atoms are removed from the surface of a chromite particle by the electrically balanced reduction of Fe^{3+} to Fe^{2+}. Further reduction will continue at the surface by the reduction of Fe^{2+} ions to the metallic state. This results in the creation of an Fe^{2+} concentration gradient between the surface and interior of the particle, causing Fe^{2+} ions to diffuse to the particle surface and leaving vacant cation sites in the unit cell. As a result of the removal of Fe^{2+}, the ratio of divalent cations to trivalent cations in the unit cell beneath the surface decreases, and the spinel becomes saturated with trivalent oxides. Hence, the removal of iron from the system can be regarded as being equivalent to the addition of trivalent cations (Cr^{3+}, Al^{3+}, and Fe^{3+}) to the spinel, which is, in fact, the same as the dissolution of the defect spinels, γ-Al_2O_3, γ-Cr_2O_3, and γ-Fe_2O_3, in the stoichiometric spinel.

There have been a number of studies on the defect structure of single spinels.[7–10] However, equilibrium constants have been established for vacancy concentrations in the spinel end member Fe_3O_4 only. Dieckmann and Schmalzried[11] determined the equilibrium constant for the oxidation equilibrium K_{ox},

$$3(Fe^{2+}) + 2/3O_2 \rightarrow 2(Fe^{3+}) + (v) + 1/3Fe_3O_4 \quad [1]$$

$$K_{ox} = \frac{e^2 h a_{mt}^{1/3}}{d^3 a_{O_2}^{2/3}} \quad [2]$$

O. SOYKAN, formerly Postgraduate Student, Department of Metallurgy and Materials Engineering, University of the Witwatersrand, is with the Soykan Mandra, Ankara, Turkey. R.H. ERIC, Acting Department Head, is with the Department of Metallurgy and Materials Engineering, University of the Witwatersrand, Johannesburg, WITS 2050, Republic of South Africa. R.P. KING, formerly with the Department of Metallurgy and Materials Engineering, University of the Witwatersrand, is with the Department of Metallurgy and Metallurgical Engineering, University of Utah, Salt Lake City, UT 84112.

Manuscript submitted July 5, 1989.

where e = the concentration of Fe^{3+} ions in the tetrahedral sites;
h = the concentration of octahedral vacancies;
a_{mt} = the ideal contribution to the activity of Fe_3O_4;
d = the concentration of tetrahedral vacancies; and
a_{O_2} = the activity of oxygen.

Interstitial cations have also been reported in mixed spinel systems as imperfections that play a part in the migration of ions.[12] Although no direct measurements have been made of the concentrations of interstitial cations in mixed spinels, indirect observations have been documented for Fe-Al spinels by Mason and Bowen.[13] Those authors[13] also reported the total concentrations of vacancies and interstitial iron as functions of oxygen activity at 1200 °C and stated that interstitial iron is predominant at low oxygen activities.

In a separate study on iron diffusion in iron-aluminate spinels at 1380 °C, Halloran and Bowen[14] found that diffusion occurred by an interstitial mechanism at low partial pressures of oxygen. They proposed that if cations were randomly distributed, interstitial iron could diffuse *via* two independent paths, *i.e.*, *via* the octahedral interstices (normally unoccupied octahedral sites in the cation sublattice), which are separated by $\sqrt{2}\ a/4$ (where a is the lattice parameter), or *via* the tetrahedral interstices, which are separated by $a/4$.

However, no experimentally derived information concerning the distribution and concentration of vacancies in mixed spinels is available at present, and the relationship of cation vacancies to temperature-dependent departures from stoichiometry is not clear and has not been investigated.

II. EXPERIMENTAL PROCEDURE

The chromite ore used in the present study was from the LG-6 layer (the sixth layer of the lower group of chromite seams) of the Bushveld Complex. The composition of the chromite and its unit-cell formula are shown in Tables I and II, respectively. The particle size range of the chromite used in the tests was −104 to +90 μm.

Finely powdered spectroscopic graphite was employed as the reductant, 30 pct in excess of the stoichiometric requirement being used to reduce iron oxide and chromium oxide to the carbide, $(Fe, Cr)_7C_3$. Although not used industrially, graphite was chosen as the reductant due to its very high purity. In this way, some side reactions that may occur, for example, because of the ash content of some coals, are avoided, which may affect the mechanism and kinetics. Loose but thoroughly mixed powders of chromite and graphite were reduced at 1416 °C in a vertical molybdenum-wound resistance furnace under an argon atmosphere. 1416 °C was chosen due to the fact that, at lower temperatures, longer periods were necessary to achieve the same reduction percentages. On the other hand, higher temperatures would result in the melting of some of the metallic products. The loss in mass of each sample was measured continuously by use of a thermogravimetric test facility incorporated in the bottom of the furnace. The mass-loss values were used for the determination of the reduction (R) by use of Eq. [3]:

$$R = \frac{\text{mass of CO evolved}}{(28/16) \times \text{mass of original removable oxygen}} \times 100 \qquad [3]$$

The removable oxygen was defined as the oxygen attached to the Cr_2O_3, FeO, and Fe_2O_3 components of the spinel. After each reduction test, a representative sample of the reaction products was split off by use of a riffle and analyzed by X-ray diffraction (XRD) techniques. The remainder was mounted in polished sections for EDAX.

X-ray diffraction analysis was carried out using a PHILIPS* X-ray diffractometer. Energy-dispersive X-ray analysis and optical examination were carried out using a JEOL 840 scanning electron microscope, which was linked to an X-ray microanalysis system. Linear point scans along a line in a particle were carried out on polished sections. This permitted concentration profiles to be constructed for chromium, iron, magnesium, aluminum, and titanium across selected cross sections. A cobalt standard was used for calibration before and after each point analysis. The results of these investigations gave a clear indication of the reactions taking place and the phases formed during the reduction.

*PHILIPS is a trademark of Philips Electronic Instruments Corporation, Mahwah, NJ.

Table I. Chemical Composition of the Chromite Ore

Component	Mass Pct
Cr_2O_3	47.50
Fe_{total}*	26.25
FeO	18.78
Fe_2O_3**	8.29
Al_2O_3	14.90
MgO	9.70
TiO_2	0.43
CaO	0.05
SiO_2	1.00

*As FeO
**Fe_{total} − FeO

Table II. Unit Cell Formula of the Chromite

Cation	Mol/32 Oxygens
Cr^{3+}	9.728
Fe^{3+}	1.569
Fe^{2+}	4.079
Al^{3+}	4.707
Mg^{2+}	3.765
Ti^{4+}	0.078
Total	23.926

III. RESULTS AND DISCUSSION

A. *Scanning Electron Microscopy and EDAX*

Energy-dispersive X-ray analysis was used in a determination of the composition of the phases formed during the reduction of chromite particles. Electron micrographs

and concentration profiles were produced for chromium, iron, aluminum, magnesium, and titanium in particles that had undergone reductions of 2.08, 7.56, 18.54, 27.48, 38.14, 44.96, 60.08, 71.67, 80.34, 91.83, and 99.05 pct. Figure 1 shows an electron micrograph of a particle after reduction of 44.96 pct. Concentration profiles for the various metals across a section of this particle are shown in Figure 2. Similar concentration profiles were obtained at all reductions up to 71.67 pct. Figures 4 through 9 summarize some of the typical experimental results obtained by EDAX.

The bright precipitates on the particle surface are iron-rich Fe-Cr carbides. Two distinct zones — an inner zone, rich in iron, and an outer zone, depleted in iron — were visible in the backscattered images of the reduced particles. After about 72 pct reduction, the inner zone disappeared. Zoning in reduced chromite grains was previously observed by Rankin,[15] who mapped the chromium and iron concentrations in reduced chromite particles from the Kroondal mine in South Africa, and by Kinloch,[16] who observed zoning in a backscattered electron image of a reduced UG-2 chromite grain. Recently, Searle and Finn,[17] who carried out a detailed electron microprobe study on reduced UG-2 chromite particles, reported similar zoning, their line scans across partially reduced chromite grains showing a marked drop in the iron concentration at the interface between the inner and outer zones. They reported that the sharp interface between the zones is reminiscent of the topochemical interface that is often observed during the reduction of single-metal oxides and also noted the presence of a sesquioxide phase, $(Cr, Al)_2O_3$, adjacent to the particle surface. This phase was also noted by Fernandes[18] and Rankin,[15] who observed that this sesquioxide formed at temperatures below 1250 °C.

The concentration profiles obtained for chromium, iron, aluminum, magnesium, and titanium during the present investigation are similar to those obtained by previous investigators. However, iron showed a concentration gradient in the outer zone. Its mass percentage decreased toward the perimeter of the particles, suggesting an outward diffusion of iron ions. The composition of the inner zone remained constant with increasing reduction, its composition being almost identical to that of the original chromite.

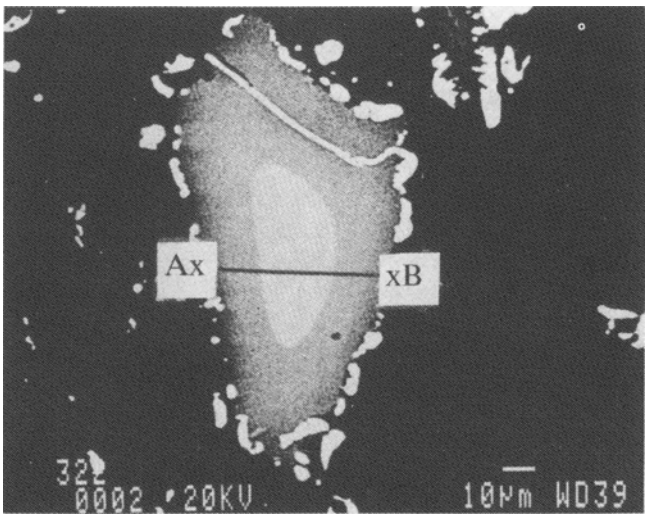

Fig. 1 — Secondary electron image of an LG-6 chromite particle after reduction by 44.96 pct at 1416 °C.

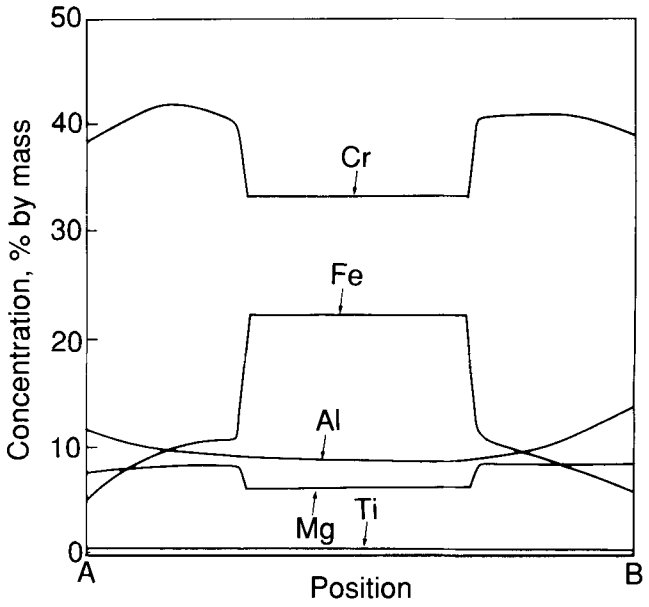

Fig. 2 — Concentration profiles along the line AB in Fig. 1.

The inner zone decreased in diameter with increasing reduction. Almost all of the iron was reduced by the time the inner zone disappeared, after which the particles exhibited porosity. This phenomenon is clearly visible in Figures 10 through 13, illustrating highly reduced particles.

B. *X-Ray Diffraction Analysis*

X-ray diffraction analysis of the unreduced chromite showed that in all of the samples, chromium is present as the mixed chromite spinels picrochromite, $(Mg, Fe) \cdot [Cr, Al]_2O_4$; aluminian chromite, $FeO \cdot (Al, Cr)_2O_3$; and donathite, $(Fe, Mg) \cdot [Cr, Fe]_2O_4$. The phases that were identified from the diffraction patterns of the reduced products are shown in Table III. All of the samples showed similar diffraction patterns. These patterns can be accepted as a reflection of the phase changes that occur at the temperature of reduction, since in an XRD analysis of quenched products, Woollacott *et al.*[19] found the quenched phases similar to those obtained at a slower cooling rate.

Although XRD analyses have indicated the presence of Fe_7C_3 phase as a reaction product from about 27.5 pct reduction, this phase was probably stabilized by dissolving a small amount of chromium. Due to the small amount of chromium, XRD analyses detected this phase as Fe_7C_3, together with the $(Cr, Fe)_7C_3$ carbide. The EDAX analyses have always indicated the presence of chromium together with iron in the metallized regions. This is illustrated in Table IV. In the mixed carbide, $(Fe, Cr)_7C_3$, the mass percent of carbon varies between 8.4 and 9.0 pct. From 27.5 pct reduction, if carbon is assumed to be the balance of the metallic carbide phase,

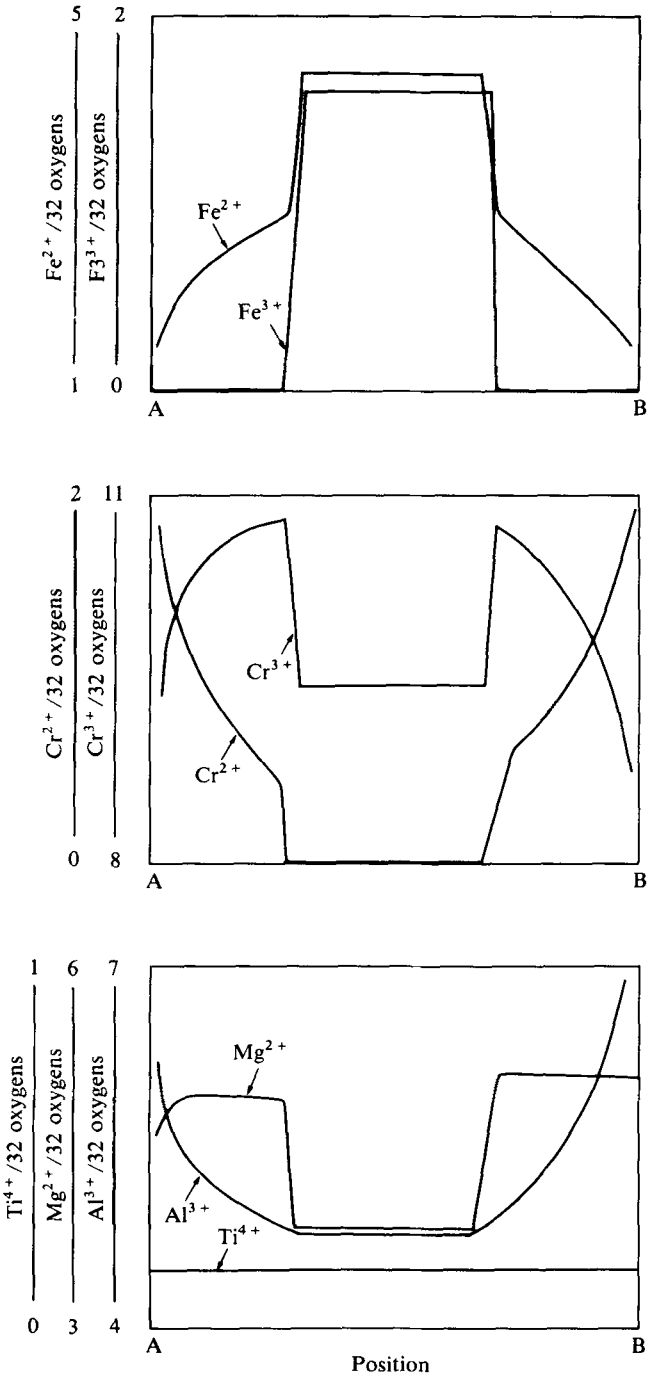

Fig. 3—Variations in the concentrations of cations across the line AB in Fig. 1.

it is seen that it changes within the above values, proving the formation of the mixed carbide.

X-ray diffraction analysis also disclosed the presence of periclase as a separate phase at reductions greater than 90 pct. Periclase was deposited as a white powder covering the surface of the charge and as white feathers at the top of the crucible. The appearance suggested strongly that a vapor-phase transport mechanism was involved in the formation of this product. In this regard, Kucukkaragoz *et al.*[20] proposed that the mechanism involves the reduction, at an extremely low partial pressure of oxygen, of magnesium ions in the spinel to magnesium vapor at

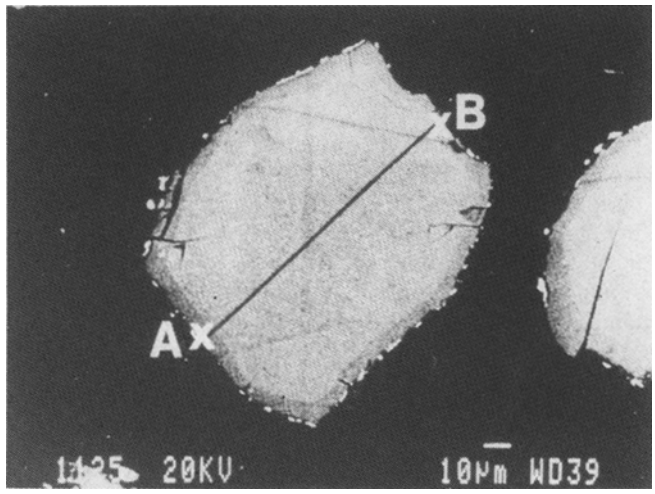

Fig. 4—Secondary electron image of an LG-6 chromite particle after reduction by 7.56 pct at 1416 °C.

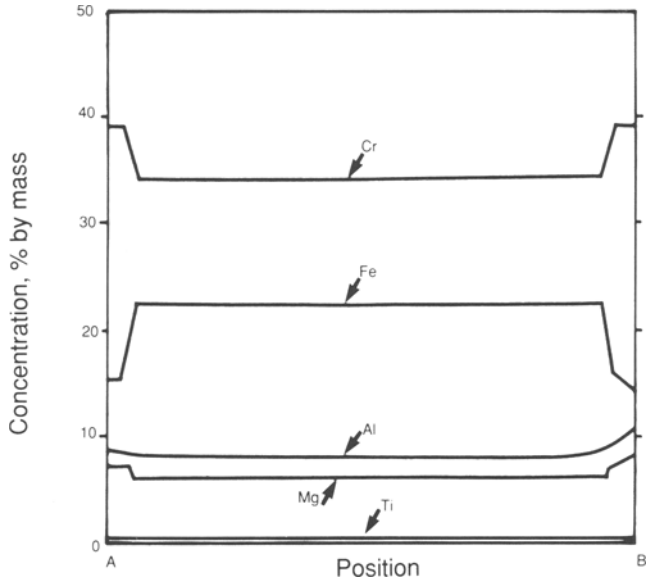

Fig. 5—Concentration profiles along the line AB in Fig. 4.

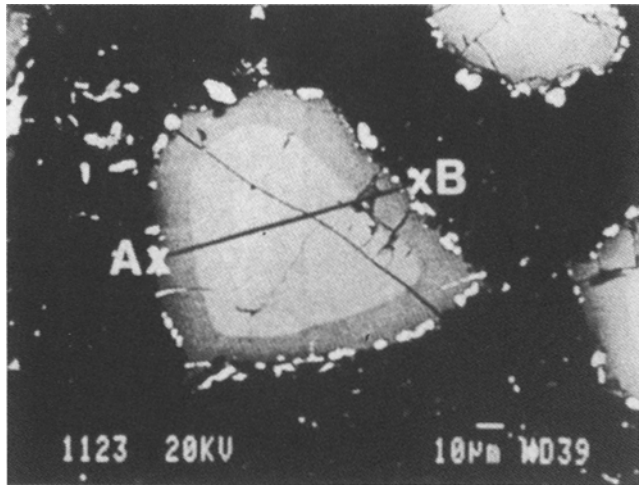

Fig. 6—Secondary electron image of an LG-6 chromite particle after reduction by 27.48 pct at 1416 °C.

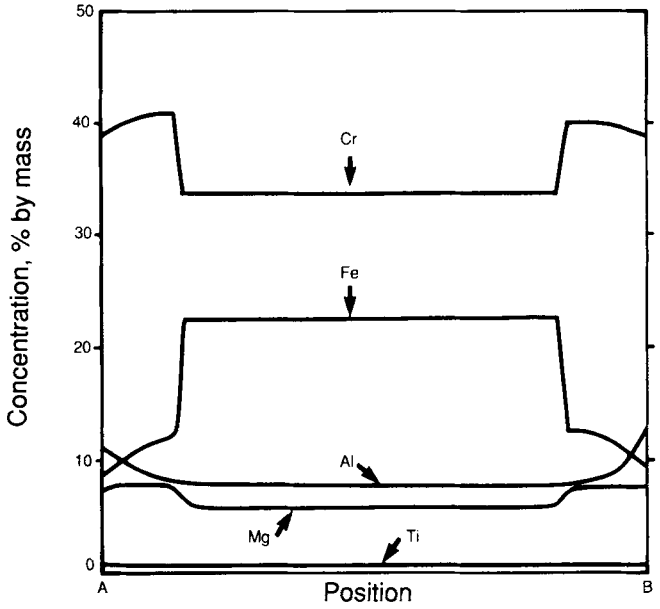

Fig. 7—Concentration profiles along the line AB in Fig. 6.

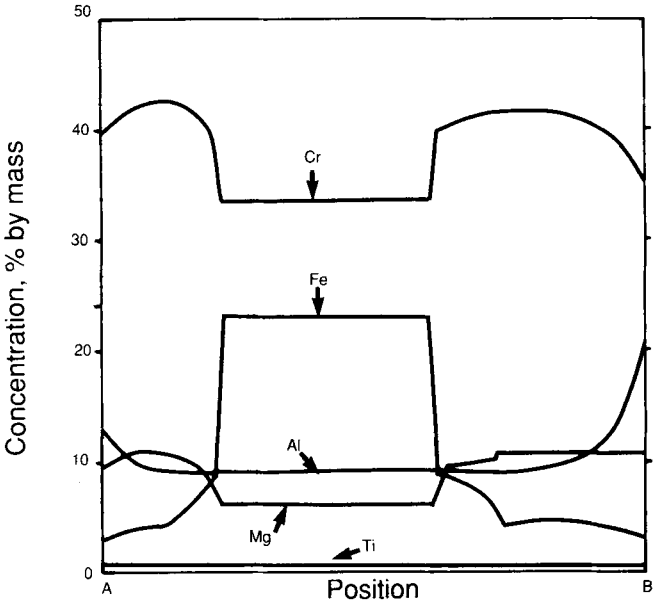

Fig. 9—Concentration profiles along line AB in Fig. 8.

the oxide-carbide interface, followed by the oxidation of this vapor to magnesium oxide at the higher oxidation potential of the gas phase.

Since the diffraction angles of many of the carbides and chromite spinel structures are very close together, a Guinier camera was used to provide higher resolution. In this way, it was possible to distinguish the diffraction angles of a new iron-depleted spinel phase that was observed coexisting with the unaltered chromite at reductions lower than 60 pct. The diffraction peaks of the new spinel phase shifted gradually in the direction of higher diffraction angle with increasing reduction, *i.e.*, with a decrease in the iron content of the spinel, while the diffraction pattern of the unreduced chromite remained unchanged but became progressively weaker. At reductions exceeding 60 pct, the diffraction angles of the new spinel phase remained stationary, coinciding with those of magnesium-chromium-aluminum spinel, and the diffraction peaks of the unreduced chromite disappeared. This phenomenon also proved that the inner and outer cores contained different phases.

IV. THE REDUCTION MECHANISM

Owing to a lack of data on defect concentrations and cation distributions in mixed spinels, the reduction mechanism at 1416 °C could not be based on the distribution of imperfections. The interpretation of data gathered from XRD analysis and EDAX was therefore based on the stoichiometry of the spinel phase. This was done as follows. The stoichiometric composition was assumed to remain constant with increasing extent of reduction, during which some of the Cr^{3+} ions were reduced to Cr^{2+}. The proposal that Cr^{2+} ions were present in the spinel was based on the observations of Ulmer and White,[1] who detected small concentrations of divalent chromium

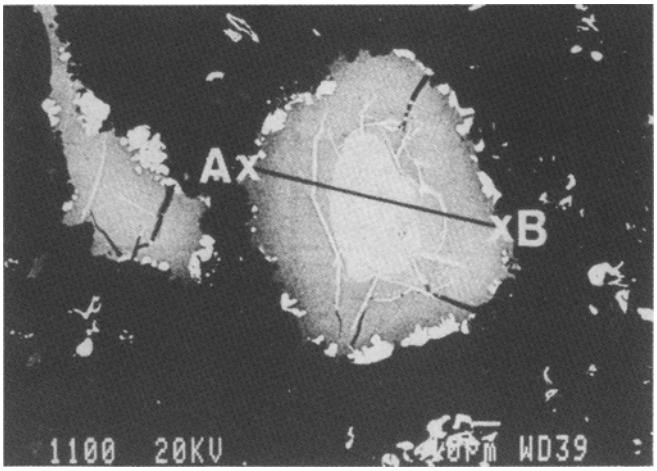

Fig. 8—Secondary electron image of an LG-6 chromite particle after reduction by 60.08 pct at 1416 °C.

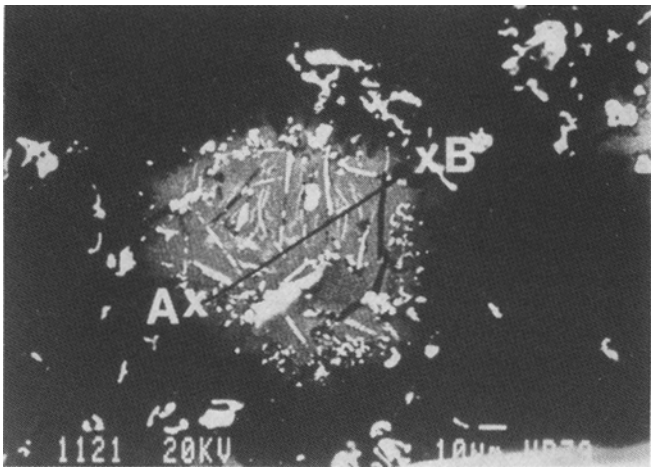

Fig. 10—Secondary electron image of an LG-6 chromite particle after reduction by 80.34 pct at 1416 °C.

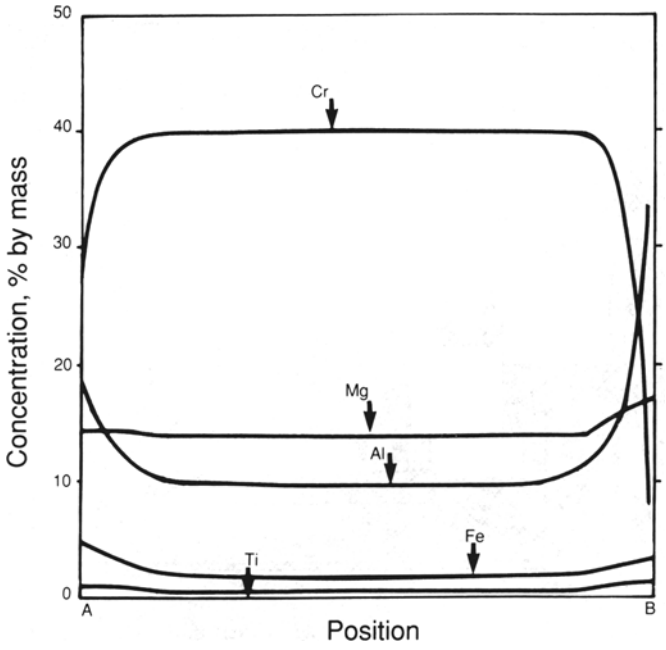

Fig. 11—Concentration profiles along line AB in Fig. 10.

ions in spinels of the $FeCr_2O_4$-$MgCr_2O_4$ solid solution series after equilibration with iron at 1300 °C.

In the present investigation, the existence of an ordered spinel structure was assumed, with Cr^{2+} ions in tetrahedral sites (when necessary), together with Mg^{2+} and Fe^{2+} ions. The calculations were based on the ideal structure of eight divalent cations, 16 trivalent cations, and 32 anions in the spinel unit cell. Any shortage of divalent cations (from chemical analyses) was compensated for by the replacement of some of the Cr^{3+} ions with Cr^{2+} ions that had been assigned to the tetrahedral sites. During the later stages of reduction, the excess divalent cations were decreased to eight by the removal of some of the Mg^{2+} from the spinel in the form of periclase (MgO). The presence of periclase as a separate phase in highly reduced chromium spinels was confirmed by

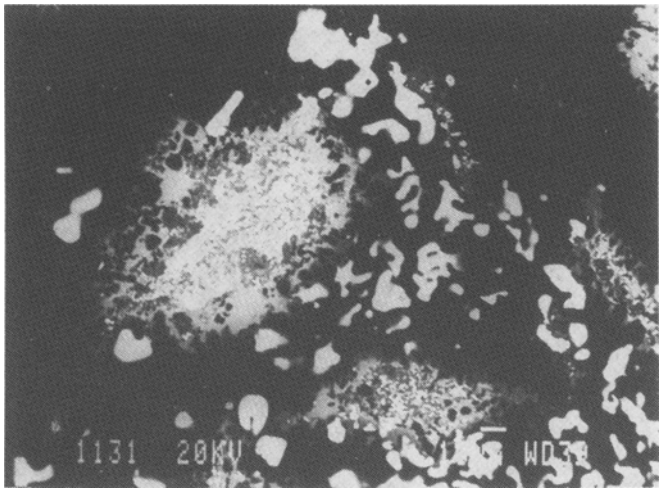

Fig. 12—Secondary electron image of an LG-6 chromite particle after reduction by 91.83 pct at 1416 °C.

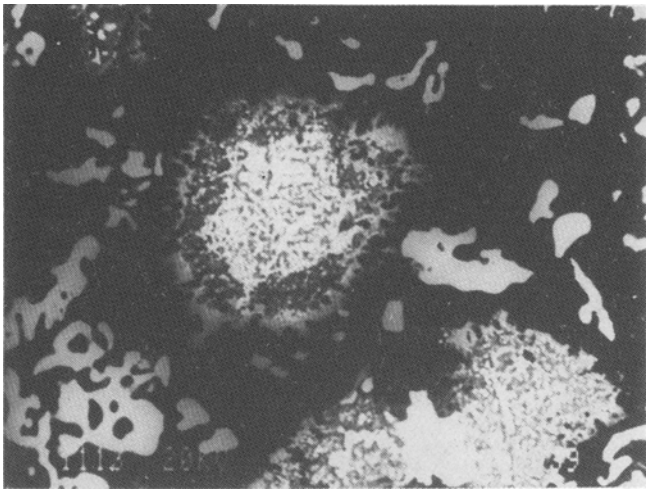

Fig. 13—Secondary electron image of an LG-6 chromite particle after reduction by 99.05 pct at 1416 °C.

X-ray analysis. The amount of oxygen in the spinel structure was determined by charge neutrality.

Figure 3 shows the variation in the number of cations per 32 oxygen atoms across a section of a particle at a reduction of 44.9 pct. The ratios of cations to oxygen ions were calculated from the EDAX data on the basis of stoichiometry and are not absolute values. Examples of the calculations are given in the Appendix. The presence of Cr^{2+} ions, up to a maximum of one Cr^{2+} ion per unit cell, in the tetrahedral sites was inferred from the EDAX results. However, the distortion that would be expected as a result was not detected by XRD analysis. Greskovich and Stubican,[21] in their studies on the influence of high temperatures on the substitution of Cr^{3+} and Cr^{2+} ions in the tetrahedral sites of $MgCr_2O_4$ spinel, found distortion in the spinel structure with increasing contents of Cr^{2+} ions and observed that the tetragonal lattice distortion (with a c/a ratio of less than unity) is formed when a critical value of approximately one Cr^{2+} ion per unit-cell formula in the tetrahedral sites is reached.

The concentration gradients (Figure 3) along the outer zone of the particle clearly show that in the earlier stages of reduction, Fe^{2+} and Cr^{3+} ions diffuse to the surface of the particle and Cr^{2+} and Al^{3+} ions diffuse toward its center. The concentration profile for Mg^{2+} ions across the outer zone is rather flat, suggesting that, compared with other ions, this species diffuses inward very rapidly. All of the cation concentration profiles obtained by EDAX up to 71.67 pct reduction showed the same trend. The inner zone of the particle, as a result, shrinks as reduction proceeds. This can be observed when the photomicrographs of Figures 1, 4, 6, and 8 are compared.

Although numerous studies have shown that oxygen is a diffusing species during the oxidation of metals,[22,23] the diffusion of oxygen in the outer zone, *i.e.*, the reaction zone, was not substantiated in the present investigation. Oxygen was therefore assumed to be an immobile species, charge neutrality being maintained by the inward diffusion of Mg^{2+} and Al^{3+} ions.

The sequence of reduction based on the analysis of the concentration profiles of the cations is described in the following sections.

Table III. Major Phases Detected by X-Ray Analysis of Reduced LG-6 Chromite at Increasing Extents of Reduction at 1416 °C

Reduction (Pct)	Phases Detected*
2.08	unaltered chromite, carbon
7.56	unaltered chromite, carbon, α-iron
18.54 25.20	picrochromite [(Fe, Mg) $(Cr, Al)_2O_4$], carbon, α-iron
27.48 38.14 44.96	picrochromite, carbon, Fe_7C_3, $(Cr, Fe)_7C_3$
60.86 64.74 71.67 76.17 80.34	$Mg(Cr, Al)_2O_4$, carbon, Fe_7C_3, $(Cr, Fe)_7C_3$, picrochromite
91.38	$Mg(Al_{1.5}, Cr_{0.5})O_4$, $MgAl_2O_4$, $(Cr, Fe)_7C_3$, Fe_7C_3, carbon
99.05	$MgAl_2O_4$, $(Cr, Fe)_7C_3$, carbon

*The phases detected are listed in order of decreasing intensity of diffraction peaks.

A. *The Reduction of Fe^{3+} and Fe^{2+} Ions in the Surface Layer*

The unit-cell formula of LG-6 chromite, the analysis of which is given in Table I, can be written as

$$(Fe_{4.08}Mg_{3.77})\,[Cr_{9.73}Al_{4.71}Fe_{1.57}Ti_{0.08}]O_{32} \qquad [4]$$

The structures of spinel solid solution series containing iron oxides have been investigated by a number of workers, notably by Verwey and Heilmann.[24] Only very slight departures from the stoichiometric spinel compositions have previously been reported. From a chemical analysis of 90 different samples of chromite from the Bushveld Complex, De Waal and Hiemstra[25] found stoichiometric compositions to a large extent. It can therefore be concluded that vacancies do not exist intrinsically as a result of the cation deficiency in the spinel lattice of the LG-6 chromite. On the assumption that all of the trivalent cations occupy 16 octahedral sites, that all of the divalent cations are in the eight tetrahedral sites, and that the substitution of Ti^{4+} results in the formation of an ulvospinel, *i.e.*, $(Me^{2+})\,[Me^{2+}, Ti^{4+}]O_4$, where Me^{2+} is Fe^{2+} or Mg^{2+}, the unit cell of LG-6 chromite can be represented by the following formula:

$$(Fe_{4.12}Mg_{3.88})\,[Cr_{9.63}Al_{4.66}Fe^{3+}_{1.55}Fe^{2+}_{0.08}Ti_{0.08}]O_{32} \qquad [5]$$

Each chromite particle can be regarded as being made up of concentric layers of unit cells of the above composition. The reduction of the unit cells situated on the surface of a particle in contact with carbon or carbon monoxide gas, or both, will be initiated by the reduction of trivalent iron to the divalent state.

$$(Fe_{4.12}Mg_{3.88})\,[Cr_{9.63}Al_{4.66}Fe^{3+}_{1.55}Fe^{2+}_{0.08}Ti_{0.08}]O_{32} + 0.775CO \rightarrow (Fe_{4.12}Mg_{3.88}) \cdot [Cr_{9.63}Al_{4.66}Fe^{2+}_{1.55}Fe^{2+}_{0.08}Ti_{0.08}]O_{31.225} + 0.775CO_2 \qquad [6]$$

This is followed by the reduction of carbon dioxide to carbon monoxide:

$$0.775CO_2 + 0.775C \rightarrow 1.55CO \qquad [7]$$

Since 0.775 oxygen ions are removed from the unit cell, the unit cell will become distorted. Therefore, in order that the spinel structure can be retained, the reduction has to be accompanied by the removal of 2.325 mole of Fe^{2+} as metallic iron.

$$(Fe_{4.12}Mg_{3.88})\,[Cr_{9.63}Al_{4.66}Fe^{2+}_{1.55}Fe^{2+}_{0.08}Ti_{0.08}]O_{31.225} + 2.325CO \rightarrow (Fe_{3.345}Mg_{3.88}) \cdot [Cr_{9.63}Al_{4.66}Fe^{2+}_{0.08}Ti_{0.08}]O_{28.9} + 2.325Fe^0 + 2.325CO_2 \qquad [8]$$

The reduction will again proceed by the distortion of the

Table IV. Element Concentrations in the Metal Phase Adjoining the Particle Surface Determined by Energy-Dispersive X-Ray Analysis at Increasing Extents of Reduction at 1416 °C

	Reduction (Pct)									
Element	7.56	18.54	27.48	38.14	44.96	60.08	71.67	80.34	91.83	99.05
Fe (Pct)	86.45	67.07	62.15	80.22	79.73	73.22	70.58	55.09	37.89	36.78
Cr (Pct)	9.38	27.10	29.43	10.64	11.26	17.95	21.04	36.07	53.02	54.76

spinel structure until all of the Fe^{2+} ions in the surface unit cells are reduced to metal *via* the reaction

$$(Fe_{3.345}Mg_{3.88})\,[Cr_{9.63}Al_{4.66}Fe^{2+}_{0.08}Ti_{0.08}]O_{28.9} + 3.425CO \rightarrow (Mg_{3.88})\,[Cr_{9.63}Al_{4.66}Ti_{0.08}]O_{25.475} + 3.425Fe^{\circ} + 3.425CO_2 \quad [9]$$

In order that the spinel structure can be built up in the surface unit cell, Reaction [9] must be accompanied by the simultaneous reduction of Cr^{3+} ions, because Al^{3+} and Mg^{2+} ions are assumed irreducible under the conditions of the tests. However, at the very later stages of reduction, the possibility of Mg^{2+} reduction exists,[20] but this does not affect the reduction model proposed here.

Cr^{3+} ions can be reduced by two possible mechanisms. If Cr^{3+} ions were reduced to metallic chromium by the reaction

$$(Mg_{3.88})\,[Cr_{9.63}Al_{4.66}Ti_{0.08}]O_{25.475} + 14.445CO \rightarrow (Mg_{2.41})\,[Al_{4.66}Mg_{0.08}Ti_{0.08}]O_{9.64} + 9.63Cr^{\circ} + 1.39MgO + 14.445CO_2 \quad [10]$$

the result would be the formation of a layer of magnesium-aluminum spinel, which would separate the iron-containing spinels from the reductant. Further reduction of the iron ions in the layers beneath the surface would be possible only if the carbon diffused through this layer. Information on the diffusion of carbon through the spinel is not available from the literature. However, Freund *et al.*[26] and Wengeler,[27] all of whom investigated the nature of the carbon in single crystals of periclase, found that carbon is capable of entering the lattice (as a result of the true thermodynamic solubility) in concentrations up to 2500 ppm or 0.25 at. pct. However, if the diffusion of carbon through the reduced layer were possible, the removal of oxygen in the form of carbon monoxide from the particles beneath the surface would cause pores to form in the reduced particles. Since the structure of the particles was dense and pore-free at reductions of almost 70 pct, this alternative was not included in the present proposed mechanism.

Alternatively, Cr^{3+} ions at the surface of the Mg-Cr-Al spinel could be reduced to the divalent state, instead of to the metal, by the reaction

$$(Mg_{3.88})\,[Cr_{9.63}Al_{4.66}Ti_{0.08}]O_{25.475} + 1.135CO \rightarrow (Mg_{3.80}Cr^{2+}_{2.28})\,[Cr_{7.35}Al_{4.66}Mg_{0.08}Ti_{0.08}]O_{24.34} + 1.135CO_2 \quad [11]$$

The Cr^{2+} ions, which diffuse inward under a Cr^{2+} concentration gradient, would reduce the Fe^{3+} ions in the unaltered chromite just beneath the surface of the particle *via* the following mechanism:

$$(Fe_{4.12}Mg_{3.88})\,[Cr_{9.63}Al_{4.66}Fe^{3+}_{1.55}Fe^{2+}_{0.08}Ti_{0.08}]O_{32} + 1.55Cr^{2+} \rightarrow (Fe_{4.12}Mg_{3.88}) \cdot [Cr_{9.63}Al_{4.66}Fe^{2+}_{1.55}Fe^{2+}_{0.08}Ti_{0.08}]O_{32} + Cr^{3+}_{1.55} \quad [12]$$

The Cr^{3+} ions, which have a very high preference for octahedral sites,[28] would then exchange places with Fe^{2+} ions in the trivalent lattice, which are very mobile compared with those in the divalent lattice. Meanwhile, owing to the presence of an iron-concentration gradient, Fe^{2+} ions would diffuse outward, becoming reduced to metallic iron.

As reduction proceeds, the replacement of 1.55 mol of Fe^{2+} ion the unit cells near the interface between the inner and outer zones would cause unit cells just inside the outer core to be enriched in chromium by 1.55 mol and to be depleted in iron by the same amount with respect to the unit cells just inside the inner core, which were found to keep their original structure with increasing reduction. Table V compares the element concentrations, which were calculated from the unit-cell formula and the experimental values determined by EDAX at points on either side of the interface between the inner and outer cores. The values are in reasonable agreement supporting the proposed mechanism.

B. *The Reduction of Fe^{2+} Ions on Tetrahedral Sites*

For the further reduction of the Fe^{2+} ions in the unit cells beneath the surface unit cell, the Cr^{2+} ions of the surface unit cell must exchange places with the Fe^{2+} ions (in the tetrahedral sites) of the unit cells just below the surface.[1,24] The formula for the unit cell just under the surface is therefore now

$$(Fe^{2+}_{4.12}Mg_{3.88})\,[Cr_{11.18}Al_{4.66}Fe_{0.08}Ti_{0.08}]O_{32} \quad [13]$$

and the formula for the surface unit cell is

$$(Mg_{3.80}Cr^{2+}_{2.28})\,[Cr_{7.35}Al_{4.66}Mg_{0.08}Ti_{0.08}]O_{24.34} \quad [14]$$

After the Cr^{2+} ions of the surface unit cell have exchanged places with the Fe^{2+} ions of the unit cell just below, the formula will be

$$(Fe_{3.12}Mg_{3.88}Cr^{2+}_{1.0})\,[Cr_{11.18}Al_{4.66}Fe_{0.08}Ti_{0.08}]O_{32} \quad [15]$$

for the unit cell immediately beneath the surface, and the formula for the surface unit cell will be

$$(Mg_{3.80}Cr^{2+}_{1.28}Fe^{2+}_{1.0})\,[Cr_{7.35}Al_{4.66}Mg_{0.08}Ti_{0.08}]O_{24.34} \quad [16]$$

The reduction of Fe^{2+} at the surface will then proceed *via* the following reaction:

$$(Mg_{3.80}Cr^{2+}_{1.28}Fe^{2+}_{1.0})\,[Cr_{7.35}Al_{4.66}Mg_{0.08}Ti_{0.08}]O_{24.34} + 1.34CO \rightarrow (Mg_{3.80}Cr^{2+}_{1.95}) \cdot [Cr_{6.68}Al_{4.66}Mg_{0.08}Ti_{0.08}]O_{23} + Fe + 1.34CO_2 \quad [17]$$

Table VI compares the element concentrations calculated from the spinel on the right-hand side of Reaction [17] with the experimental values determined by EDAX when the reduction of iron was nearly complete and the particle contained no inner core. The agreement is good.

C. *The Reduction of Chromium Ions*

Once the divalent iron has been completely reduced, the spinel consists of a magnesium-chromium-aluminum

Table V. Assayed and Calculated Concentrations of Various Elements at the Inner and Outer Zones*

	Cr		Fe		Al		Mg		Ti	
Zone	Assay	Calculated	Assay	Calculated	Assay	Calculated	Assay	Calculated	Assay	Calculated
Reduction 27.48 Pct										
Outer	39.86	37.46	12.07	15.12	8.01	8.10	7.61	6.08	0.53	0.25
Inner	33.62	32.15	22.56	20.61	7.88	8.07	6.13	6.05	0.43	0.24
Reduction 38.14 Pct										
Outer	40.30	37.46	10.89	15.12	8.94	8.10	8.58	6.08	0.45	0.25
Inner	33.68	32.15	22.64	20.61	8.36	8.07	6.09	6.05	0.41	0.24

*All concentrations are expressed as percentages by mass.

spinel phase, as seen in Reaction [17]. The trivalent, and any divalent, chromium ions present are reduced to metal step-by-step by the reductant at the surface, while the stoichiometry of the spinel structure is retained; *i.e.*,

$$(Mg_{3.80}Cr^{2+}_{1.95})\,[Cr_{6.68}Al_{4.66}Mg_{0.08}Ti_{0.08}]O_{23} + 1.32CO \rightarrow (Mg_{3.80}Cr^{2+}_{1.62})\,[Cr_{6.02}Al_{4.66}Mg_{0.08}Ti_{0.08}]O_{21.68} + 0.99Cr^{\circ} + 1.32CO_2 \quad [18]$$

As the ratio of Al^{3+} to Cr^{3+} ions is larger in the surface unit cells, there will be an inward diffusion of Al^{3+} and an outward diffusion of Cr^{3+} ions. The final reduction product will be a Mg-Al spinel phase and MgO if the maximum solubility of MgO in the spinel phase is exceeded, *i.e.*,

$$(Mg_{2.41})\,[Al_{4.66}Mg_{0.08}Ti_{0.08}]O_{9.64} \quad [19]$$

In each of the stages described above, oxygen was removed from the surface. This mechanism is similar to that described for the reduction of iron ores.[29,30] It is obvious that the above mechanism, which is described stagewise, occurs simultaneously, and that metallized iron and chromium are present as their carbides, as determined by XRD of the reduced products.

V. SUMMARY AND CONCLUSIONS

The main objective of this work was the study of the mechanism of reduction of chromite by graphite. This was investigated in detail by mineralogical examination of the reduced samples and the phases resulting from the reduction process. The morphological and compositional changes occurring during the reduction were identified and related to the specific stages of the reduction. The reduction was shown to occur by the outward diffusion of Fe^{2+} and Cr^{3+} ions, and the inward diffusion of Cr^{2+}, Al^{3+}, and Mg^{2+} ions, through the outer zones of the particles. In essence, the chromite becomes deficient in iron and chromium owing to the diffusion of these elements and the formation of Fe-Cr carbides. The diffusion of magnesium and aluminum results in shrinkage of the chromite grains.

Table VI. Assayed and Calculated Concentrations of the Various Elements When the Reduction of Iron is Complete at a Reduction of 71.67 Pct

Element	Assay, Pct (by Mass)	Calculated, Pct (by Mass)
Cr	43.82	43.12
Fe	2.52	00.00
Al	10.01	12.08
Mg	11.94	9.06
Ti	0.62	0.36

The results of the investigation can be summarized as follows.

1. Drastic morphological and compositional changes occur during the reduction. During the initial stages of the process, metal nuclei form at the perimeter of the particle. Later, an inner zone, consisting of unreduced chromite, becomes visible. This zone shrinks and disappears at a reduction of about 70 to 75 pct. During the final stages of the process, at a reduction greater than 75 pct, the massive, dense particle changes completely and becomes a disintegrated, porous structure.
2. Mineralogical examination of partially reduced chromite particles suggested the following mechanism for the reduction of LG-6 chromite at 1416 °C. The reduction sequence of chromite was explained on the basis of the constant stoichiometry of the spinel phase with increasing reduction and a spinel unit-cell concept. Initially, the Fe^{3+} ions in the unit cells at the surface of the chromite particle are reduced to the divalent state. Immediately afterward, the Fe^{2+} ions are reduced to the metallic state, and the Cr^{3+} ions are reduced to the divalent state. Concentration profiles of the cations comprising the spinel unit cell were drawn from EDAX data. The concentration gradients of the Fe^{2+}, Cr^{2+}, Cr^{3+}, Mg^{2+}, and Al^{3+} ions provided the driving force for the diffusion of these ions. The further reduction of the spinel unit cells beneath the surface of the particle proceeds by the inward diffusion of Cr^{2+} ions, which reduce the Fe^{3+} ions to the divalent state. As a result, the particle becomes zoned, consisting of an inner core with the composition of the original chromite and an iron-depleted outer zone from which the Fe^{3+} component has been removed. The final product of the reduction is an iron- and chromium-free spinel, $MgAl_2O_4$.
3. The proposed mechanism is specific to the reduction of LG-6 chromite by graphite, and further data are needed before it can be applied to the reduction of chromites in general.

APPENDIX

Calculation of the Number of Cations per 32 Oxygen Ions from EDAX Analyses

A. *Outer Zone of a Partially (44.96 Pct) Reduced Chromite Particle*

The point analysis of the outer zone was as follows.

$W_{Cr} = 38.72$
$W_{Fe} = 6.1$
$W_{Ti} = 0.52$
$W_{Al} = 11.34$
$W_{Mg} = 7.68$
$W_O = 35.63$
Total 100.00

where W is the percentage (by mass) of each element.

The atomic fraction (N) of the elements can be calculated from the point analysis by use of the following formula:

$$N_{Cr} = (W_{Cr}/M_{Cr})/[(W_{Cr}/M_{Cr}) + (W_{Fe}/M_{Fe}) + (W_{Ti}/M_{Ti}) + (W_{Al}/M_{Al}) + (W_{Mg}/M_{Mg}) + (W_O/M_O)]$$

where the M's are the respective atomic weights.

In the following example,

$$N_{Cr} = 0.745/(0.745 + 0.109 + 0.011 + 0.420 + 0.316 + 2.227) = 0.195 \text{ and, similarly,}$$

$N_{Fe} = 0.028$

$N_{Ti} = 0.003$

$N_{Al} = 0.110$

$N_{Mg} = 0.082$

$N_O = 0.582$

The number of cations per 32 oxygen ions can be calculated from their atomic fractions and normalized by being multiplied by 24/22.98, as follows:

$(N_{Cr}/N_O) \times 32 = 10.72 \times 24/22.98 = 11.20$
$(N_{Fe}/N_O) \times 32 = 1.54 \times 24/22.98 = 1.61$
$(N_{Ti}/N_O) \times 32 = 0.16 \times 24/22.98 = 0.17$
$(N_{Al}/N_O) \times 32 = 6.05 \times 24/22.98 = 6.32$
$(N_{Mg}/N_O) \times 32 = 4.51 \times 24/22.98 = 4.71$
$22.98 \times 24/22.98 = 24.00$

The results were normalized to 24 cations, since it was assumed that eight tetrahedral sites and 16 octahedral sites are occupied by cations.

Since the substitution of Ti^{4+} ions results in the ulvospinel structure, the divalent cations present in the tetrahedral sites are as follows:

Fe^{2+} in tetrahedral sites = 1.61 − 0.17 = 1.44;
$Fe^{2+} + Mg^{2+}$ in tetrahedral sites = 1.44 + 4.71 = 6.15;
Cr^{2+} in tetrahedral sites = 8.00 − 6.15 = 1.85;
Cr^{3+} in octahedral sites = 11.19 − 1.85 = 9.34; and
Fe^{2+} in octahedral sites = 0.17.

Consequently, the formula of the spinel is

$$(Mg_{4.71}Cr_{1.85}Fe_{1.44})\,[Cr_{9.34}Al_{6.32}Fe^{2+}_{0.17}Ti_{0.17}]O_{32}$$

where the parentheses and the brackets refer to tetrahedral and octahedral coordination, respectively.

B. *Inner Core of a Partially Reduced (44.96 Pct) Chromite Particle*

By the method used above, the number of cations per 32 oxygens can be calculated from their atomic fractions and normalized by being multiplied by 24/29.23 as follows:

$(N_{Cr}/N_O) \times 32 = 11.50 \times 24/29.23 = 9.44$
$(N_{Fe}/N_O) \times 32 = 7.19 \times 24/29.23 = 5.90$
$(N_{Ti}/N_O) \times 32 = 0.15 \times 24/29.23 = 0.12$
$(N_{Al}/N_O) \times 32 = 5.80 \times 24/29.23 = 4.76$
$(N_{Mg}/N_O) \times 32 = 4.59 \times 24/29.23 = 3.77$
$29.23 \qquad 24.00$

Fe^{2+} in octahedral sites = 0.12;
Fe^{3+} in octahedral sites = [(5.90 − 0.12) + 3.77] − 8 = 1.55; and
Fe^{2+} in tetrahedral sites = 5.78 − 1.55 = 4.23.

Consequently, the formula of the spinel is

$$(Fe_{4.23}Mg_{3.77})\,[Cr_{9.44}Al_{4.76}Fe^{3+}_{1.55}Fe^{2+}_{0.12}Ti_{0.12}]O_{32}$$

where the parentheses and the brackets refer to tetrahedral and octahedral coordination, respectively.

ACKNOWLEDGMENTS

This paper is published by permission of the Council for Mineral Technology (Mintek) and the Ferro Alloy Producers' Association of South Africa. The authors are deeply grateful to both of these organizations for their financial support.

REFERENCES

1. G.C. Ulmer and W.B. White: *J. Am. Ceram. Soc.*, 1966, vol. 49 (1), pp. 50-51.
2. R.W.G. Wyckoff: *Crystal Structures*, 2nd ed., Interscience Publishing Co., New York, NY, 1962, vol. 3, pp. 77-78.
3. K.P.D. Perry: Ph.D. Thesis, University of the Witwatersrand, Johannesburg, Republic of South Africa, 1986.
4. F.A. Kroger: *The Chemistry of Imperfect Crystals*, 2nd ed., North-Holland/American Elsevier, Amsterdam, The Netherlands, 1974, vol. 2, pp. 251-55.
5. J.E. Castle and P.L. Surman: *J. Phys. Chem.*, 1967, vol. 71, pp. 4255-59.
6. W.D. Kingery, D.C. Hill, and R.P. Nelson: *J. Am. Ceram. Soc.*, 1960, vol. 43 (9), pp. 473-76.
7. E.J.M. Verwey: *Z. Kristallogr.*, 1935, vol. 91, pp. 65-69.
8. E. Kordes: *Z. Kristallogr.*, 1935, vol. 91, pp. 193-228.
9. G. Kullerud, G. Donnay, and J.D.H. Donnay: *1968 Year Book*, Carnegie Institute, Washington, DC, vol. 66, pp. 497-98.
10. G. Kullerud, G. Donnay, and J.D.H. Donnay: *Z. Kristallogr.*, 1969, vol. 128 (1–2), pp. 1-17.
11. R. Dieckmann and H. Schmalzried: *Ber. Bunsen-Ges. Phys. Chem.*, 1977, vol. 81 (4), pp. 414-19.
12. W. Mueller and H. Schmalzried: *Ber. Bunsen-Ges. Phys. Chem.*, 1964, vol. 68 (3), pp. 270-76.
13. T.O. Mason and H.K. Bowen: *J. Am. Ceram. Soc.*, 1981, vol. 64 (2), pp. 86-90.
14. J.W. Halloran and H.K. Bowen: *J. Am. Ceram. Soc.*, 1980, vol. 63 (1–2), pp. 58-65.

15. W.J. Rankin: *Arch. Eisenhuettenwes.*, 1979, vol. 50 (9), pp. 373-78.
16. E.D. Kinloch: in *ICAM 81*, Proc. 1st Int. Congress on Applied Mineralogy, J.P.R. de Villiers and P.A. Cawthorn, eds., The Geological Society of South Africa, Johannesburg, Republic of South Africa, 1983, pp. 337-49.
17. M.J. Searle and C.W.P. Finn: Report No. M96, Council for Mineral Technology, Randburg, Republic of South Africa, 1984.
18. T.R.C. Fernandes: in *MINTEK 50*, Proc. Int. Conf. on Mineral Science and Technology, L.F. Haughton, ed., Council for Mineral Technology, Randburg, Republic of South Africa, 1985, vol. 2, pp. 913-22.
19. N.L. Woollacott: Report No. 1950, National Institute for Metallurgy, Randburg, Republic of South Africa, 1978.
20. C.S. Kucukkaragoz, S.H. Algie, and C.W.P. Finn: MINTEK Report No. M154, Council for Mineral Technology, Randburg, Republic of South Africa, 1984.
21. C. Greskovich and V.S. Stubican: *J. Phys. Chem. Solids*, 1966, vol. 27, pp. 1379-84.
22. A. Novakova, C. Kleir, and J.S. Jiru: in *Reactivity of Solids*, G.M. Schwab, ed., Elsevier, New York, NY, 1965, pp. 269-76.
23. O. Katsutoshi and S. Awazu: *J. Phys. Chem. Solids*, 1968, vol. 29, pp. 1269-73.
24. E.J.W. Verwey and E.L. Heilmann: *J. Chem. Phys.*, 1947, vol. 15, pp. 174-80.
25. S.A. De Waal and S.A. Hiemstra: Report No. 1709, National Institute for Metallurgy, Randburg, Republic of South Africa, 1975.
26. F. Freund, H. Kathrein, H. Wengeler, R. Knobel, and H.J. Heinen: *Geochim. Cosmochim. Acta*, 1980, vol. 44, pp. 1319-33.
27. H. Wengeler: Ph.D. Thesis, University of Cologne, Cologne, Federal Republic of Germany, 1980.
28. A. Navrotsky and O.J. Kleppa: *J. Inorg. Nucl. Chem.*, 1967, vol. 29, pp. 2701-14.
29. J.O. Edstrom: *J. Iron Steel Inst.*, 1953, vol. 175, pp. 289-304.
30. J.O. Edstrom: *Jernkontorets Ann. 141*, 1957, vol. 12, pp. 809-31.